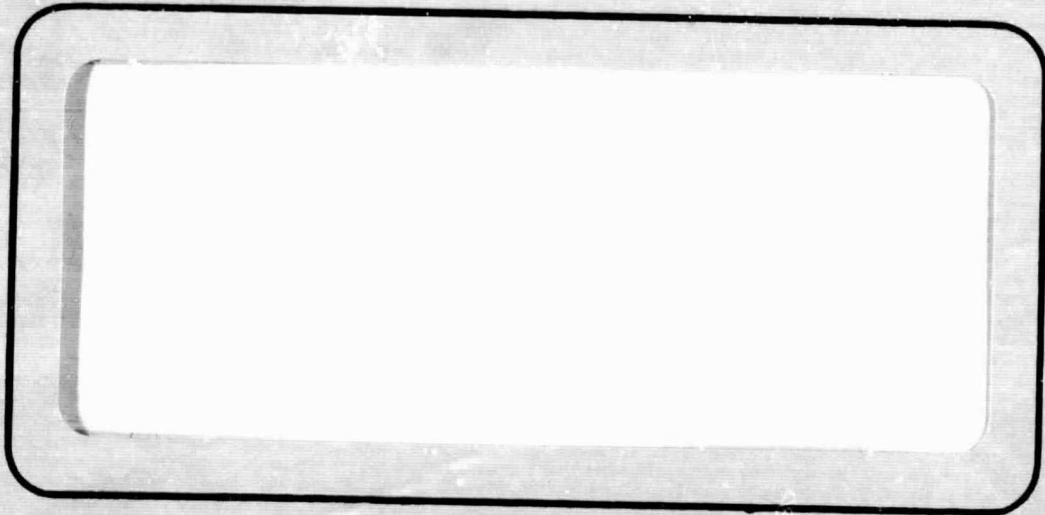


General Disclaimer

One or more of the Following Statements may affect this Document

- This document has been reproduced from the best copy furnished by the organizational source. It is being released in the interest of making available as much information as possible.
- This document may contain data, which exceeds the sheet parameters. It was furnished in this condition by the organizational source and is the best copy available.
- This document may contain tone-on-tone or color graphs, charts and/or pictures, which have been reproduced in black and white.
- This document is paginated as submitted by the original source.
- Portions of this document are not fully legible due to the historical nature of some of the material. However, it is the best reproduction available from the original submission.

NASA-STIC



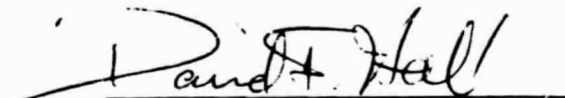
TRW
SYSTEMS GROUP

ONE SPACE PARK • REDONDO BEACH, CALIFORNIA

FACILITY FORM 802	N69-35539	
	(ACCESSION NUMBER)	(THRU)
	40	1
	(PAGES)	(CODE)
	NR-105316	31
	(NASA CR OR TRX OR AD NUMBER)	(CATEGORY)

First Quarterly Technical Report
PROPULSION BEAM DIVERGENCE EFFECTS

Contract No. 952350



David F. Hall
Program Manager

This work was performed for the Jet Propulsion Laboratory,
California Institute of Technology, sponsored by the
National Aeronautics and Space Administration under
Contract NAS7-100.

TRW Systems
One Space Park
Redondo Beach, California

15 May 1969

ABSTRACT

The second phase of a program to develop understanding of and tolerance-level criteria for the deleterious effects of electrostatic rocket exhaust (Cs , Cs^+ , Hg , Hg^+) impinging on typical classes of spacecraft surfaces is underway. Prior work was done under Contract No. NAS7-575. This phase includes fabrication of necessary experimental fixtures and exploratory experiments. The current status of fixture design, fabrication, and testing is reported along with early results of exposures of Kapton to Cs and soft solder to Hg .

This report contains information prepared by TRW Systems under JPL subcontract. Its content is not necessarily endorsed by the Jet Propulsion Laboratory, California Institute of Technology, or the National Aeronautics and Space Administration.

TECHNICAL CONTRIBUTORS

Electric Propulsion Technology

D. F. Hall

Thermophysics

L. Kelley

Metallurgy

R. Mendelson

Chemistry

R. Meyers

I. INTRODUCTION

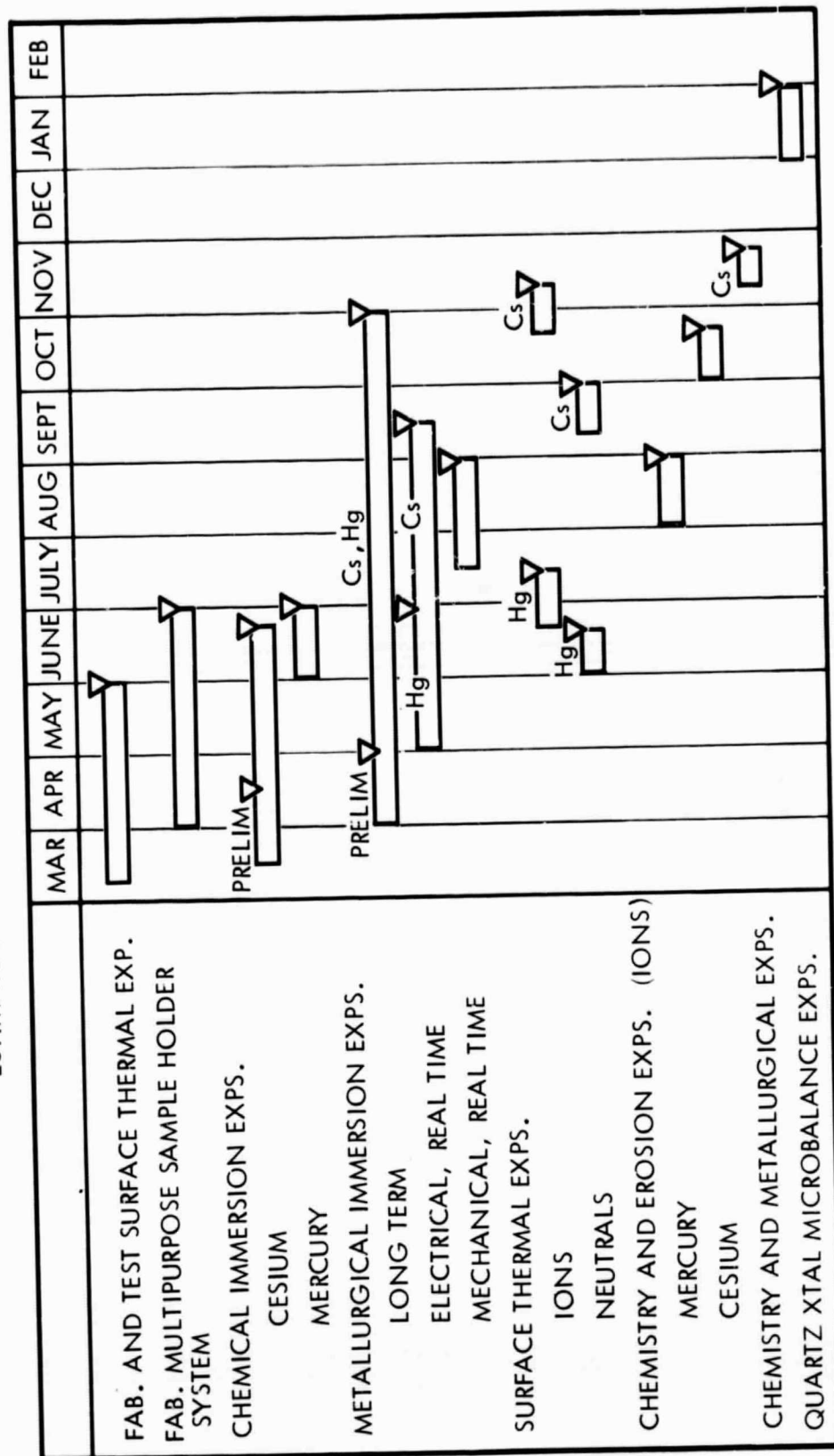
Electrostatic rockets emit propellant particles into at least 2π steradians. Spacecraft (S/C) designers therefore require tolerance-level criteria for the almost inevitable interception of propellant particles by S/C surfaces. Under contract NAS7-575 a systematic analytical study was made of the deleterious effects of Hg, Hg^+ , Cs, and Cs^+ on spacecraft surfaces. (1-5) Erosion of non-metallic surfaces by sputtering, degradation of thermal control coatings, chemical degradation of non-metallic surfaces, and condensation on solar cell cover glasses are expected to pose the most restrictive design constraints. Of the above areas, quantitative constraints have been generated for condensation; the others are at the qualitative stage and require experimental study.

The program goals of the present effort are 1) to fabricate experimental fixtures required to make these measurements, and 2) perform exploratory experiments to determine in which areas future emphasis should lie.

The program contains four work units; Metallurgy, Chemistry, Thermophysics, and Electric Propulsion Technology. The metallurgy group is charged with elucidating reactions between the propellants and S/C metals. The chemistry group is responsible for elucidating reactions between the rocket efflux and non-metallic S/C materials. The thermophysics group will determine the surface thermal changes which occur in various thermal control coatings. The electric propulsion group is responsible for sputtering experiments, operation of the primary facility in which most exposures are made, and program management.

An Estimated Schedule of Experimental Activities was compiled and appears on the following page. The schedule is regarded as tentative, since early results may well dictate a shift in program emphasis. The schedule reflects the current scientific priorities, as determined by the JPL Contract Manager. They are as follows:

ESTIMATED SCHEDULE OF EXPERIMENTAL ACTIVITIES



<u>Priority</u>	<u>Experiments</u>
1	Chemistry
1	Thermophysics
2	Erosion (sputtering)
2	Metallurgy
3	Electrical
4	QCM (sputtering)

The immersion tests referred to in the schedule consist of submerging S/C material samples in the liquid propellants. This is a relatively simple way to explore reactions and reaction rates under conditions simulating very high propellant arrival rates. The other experiments are to be performed in conditions which simulate the space environment.

II. TECHNICAL DISCUSSION

A. Electric Propulsion Technology

1. Dispersal of Information. Highlights of the knowledge gained on NAS7-575 were presented to the electric propulsion community. AIAA Paper No. 69-271, "Electrostatic Rocket Exhaust Effects on Solar-Electric Spacecraft Subsystems" was given at the AIAA 7th Electric Propulsion Conference. TRW bore the costs associated with this presentation. The paper was subsequently submitted to the Journal of Spacecraft and Rockets for possible archival publication.

Technical progress reports were issued for the months of February and March.

2. Facilities. An oil vapor trap was installed in the roughing line of the 4 x 8 foot tank. Its purpose is to prevent roughing pump oil from reaching the experimental chamber.

A large leak in the vacuum chamber, mentioned last month, was repaired.

A sophisticated digital set point temperature controller was installed in the thruster console for boiler temperature control. The instrument must

operate at thruster screen potential (approximately 3 KV). It passed a hi-pot test at 6 KV. Its successful operation is described under Section 4 below.

The rear section of the 4 x 8 chamber was painted with two coats of 3M 401-C10 black paint for the in situ surface thermal experiments.

A special table was constructed to permit accurate positioning and indexing of the xenon lamp with respect to the 4 x 8 chamber. Provision has been made for exhausting from the lab ozone produced by the lamp.

It will be desirable to begin and terminate sample exposures quickly. However, the engine boiler system has an appreciable thermal time constant. Therefore a mechanical engine shutter has been designed and fabricated which may be interposed between the engine and the samples.

3. Multipurpose Sample Holder. The multipurpose sample holder concept is shown in Figure 1. It has a large sample capacity, sample temperature control, shielded areas on each sample for erosion depth measurements, a multiplicity of sample orientations with respect to an incident beam, and provision for making negligible the incidence of foreign particles on sample surfaces. Therefore the holder will be suitable for erosion depth measurements as a function of angle, and exposure of both metallic and nonmetallic samples to ion and atom beams as a function of temperature for chemical and metallurgical investigations. These design features are discussed in more detail in Ref. 4.

In addition to the above requirements, provision is being made for removing the sample holder in an inert atmosphere following cesium beam exposures. Figure 2 shows how this is to be accomplished.

The sample holder, mounted on a port plate is loaded behind the square cutout in the collector. To facilitate the insertion and positioning of the sample holder, a horizontal track will be installed in the tank. When it comes time to remove the assembly, a large glove bag is attached to the port and a support table positioned adjacent. The assembly is rolled out

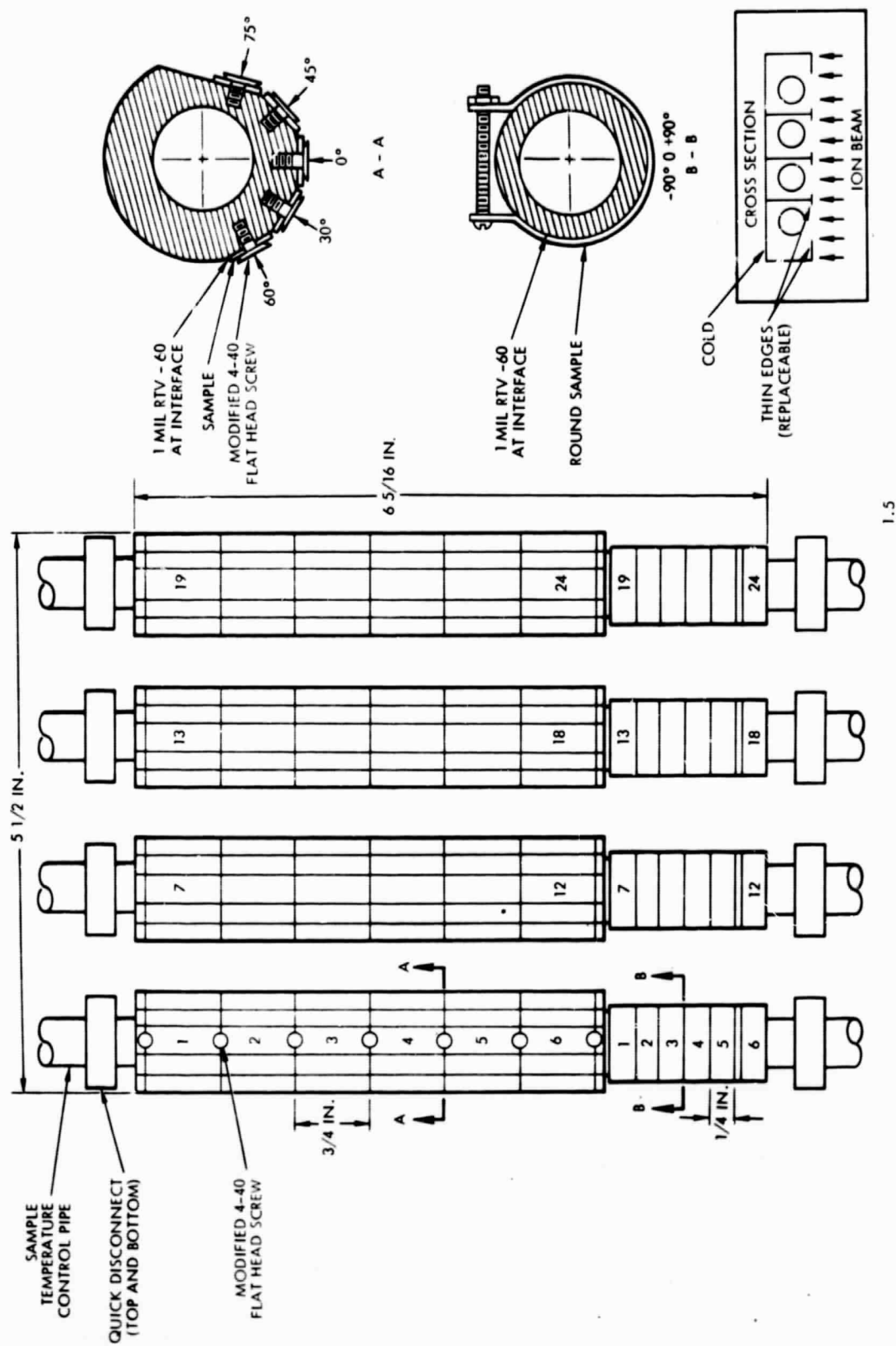


Figure 1. Conceptual design of multipurpose sample holder.

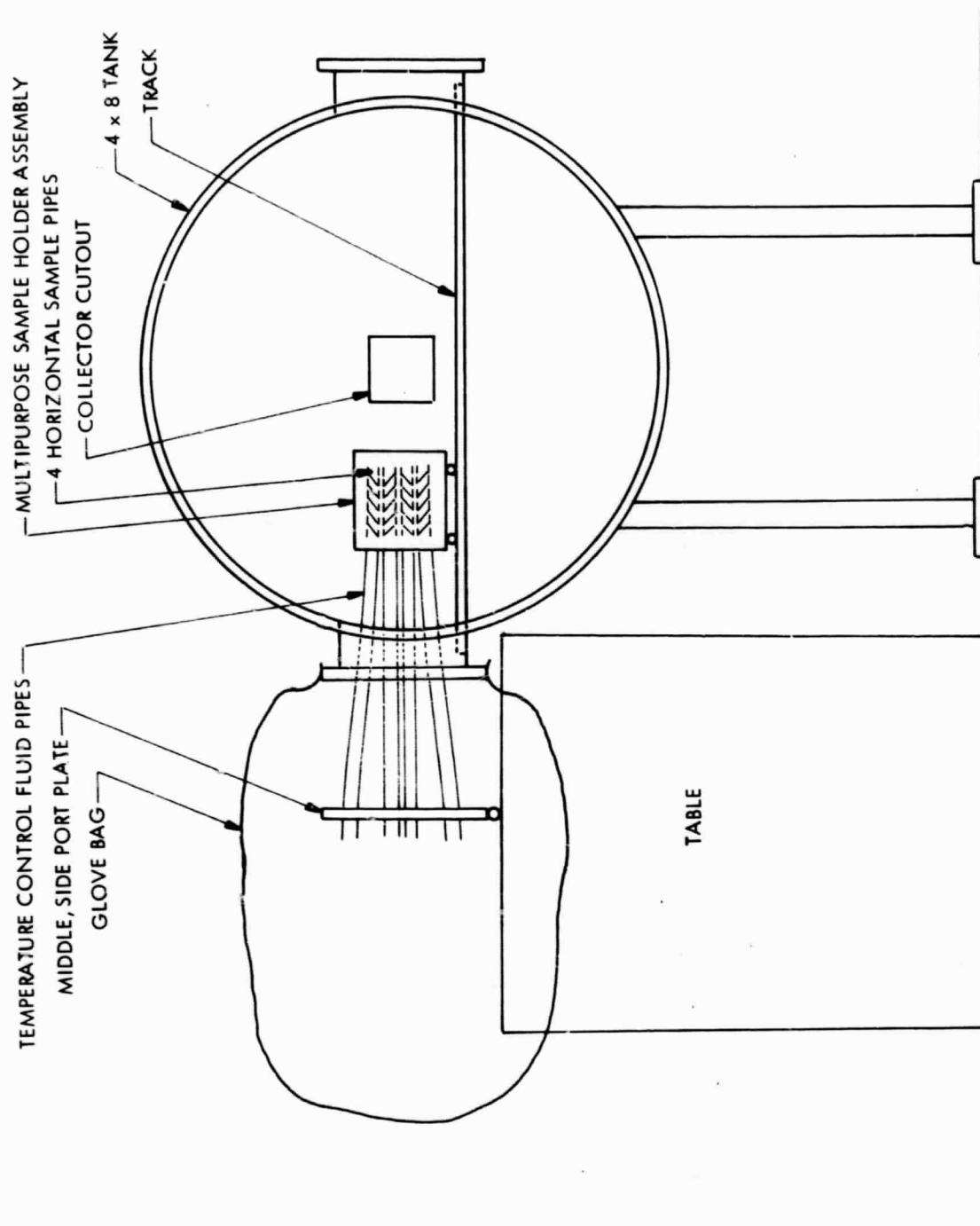


Figure 2. Scheme for removing multipurpose sample holder into inert atmosphere. (Viewed from rear of chamber.)

on the internal track and table until its entirely within the glove bag. Then the four sample containing pipes are disconnected and placed in an air tight transfer box and carried to a nearby glove box. In the glove box the samples are demounted from the pipes and measurements begun.

During the reporting period, effort was expended in finalizing the many design details of the sample holder. Most of these details interact with each other, so an interactive process is required. In addition to the aspects of sample holder positioning and removal, discussed above, attention has been focused in the following areas.

- a. Obtaining good registration of sample pipes in the holder.
- b. Easy removability of sample pipes without endangering samples.
- c. Avoidance of thermal shorts between sample pipes.
- d. Location and cooling of sputtering shields.
- e. Sample substrate design and providing reference surfaces for erosion depth measurements.
- f. Compatibility of the system with the surface thermal sample holder system.

The various aspects of the system are in different stages of completion. The flat sample substrate design has been finalized (area e above), and an initial batch of 200 manufactured. The collector mounted sputtering shield design is complete. A construction concept meeting constraints (a), (b), and (c) has been evolved and detailed design is now in progress.

4. Measurements. The building water temperature was recorded as a function of time for the Thermophysics Group to allow evaluation of a proposed simplification in the sample holder design.

Between 0900, 2/19 and 1720, 3/2, the water was always between 18 and 20°C. More important, the highest time rate of temperature change observed was 1.6°C/hr and that was atypical. Typically, during working hours, the temperature was constant within $\pm 0.5^\circ\text{C}$ and time rates of change were less than 0.5°C/hr.

Six gravimetric boiler calibration runs were made with mercury to establish the relationship between boiler temperature controller set-point and mass flow. Knowledge of this relationship permits setting neutral particle arrival rates at the same location when the thruster is used as an atomic oven, and estimating neutral fraction when the thruster is accelerating ions.

This data is shown in Figure 3. The vertical confidence bars represent weighing and "end effect" (finite run start and stop periods) errors, while the horizontal bars represent the controller dead band ($\pm 10 \mu V \approx \pm 0.2^\circ C$).

The reason for the "bad" data point at set-point 6.36 is not known. This was the first run made, and inadequate run length is responsible for the large error bars ($\pm 18\%$). One hypothesis is that the surface of the mercury in the boiler was oxidized and therefore its vapor pressure lowered. An additional data point will be sought in this region of the calibration curve. (To achieve the desired precision, a gravimetric run must expel at least 50 gms of propellant, so low flow rate runs are quite long.)

B. Metallurgy

1. Summary. During the first quarterly reporting period, test vessels for the immersion tests of the various test materials have been designed and fabricated. These test vessels are compatible with the cesium distilling apparatus described under Chemistry, and will be used for both the mercury and cesium immersion tests. During the reporting period the immersion test of the 63 w/o tin solder was initiated.

a. Test Vessel Design. The test vessel that is used for the immersion tests is essentially a test tube which provides a sealed test chamber. Figure 4 shows the vessel design. The glass rod in the center of the chamber provides a viewing platform on which the sample sits when the tube is inverted. In the mercury immersion tests, the rod insures that the sample will remain submerged.

b. Experimental Procedure. The solder used for the immersion tests was a rosen core 63 w/o Sn solder. The solder was cast into a cylindrical shape 0.4900" in diameter in a quartz test tube. The solder was then remelted under an argon atmosphere in an induction furnace. The solder was kept molten long enough to allow the bulk of the rosen to float to the top of the liquid pool. After the solder solidified samples were taken from the lower half of the remelted section. No residual rosen was observed on the cut sample. The solder sample was then ground so that both ends were flat, solvent cleaned, weighed, and measured. The sample was then placed in the cleaned test vessel and the glass was sealed. Figure 5a is a photograph of the sample in the sealed test vessel. Fifty grams of triple distilled mercury was then added to the test vessel through the glass valve. The test vessel was placed in a vertical position so that the mercury completely covered the solder sample.

c. Observations. Upon addition of the mercury to the test vessel, an immediate surface reaction with the solder seemed to take place. The surface appeared to be completely wet by the mercury. Examination of the solder sample was performed on a daily basis for one week. During this time an increasing amount of solder was dissolved from the original sample. After 2 days a precipitate was seen at the upper end of the test vessel. Figures 5b and 6 show the test vessel after 1 week of exposure. At this point the sample was eroded quite severely but still had the shape of a cylinder. Examination of the equilibrium diagrams of a lead/mercury and tin/mercury revealed that the liquid mercury will hold only about 1 to 2% of either constituent in solution so that the precipitated material would be expected. After the first week of exposure the reaction rate seemed to slow considerably. After two additional weeks no further change could be seen in the solder sample.

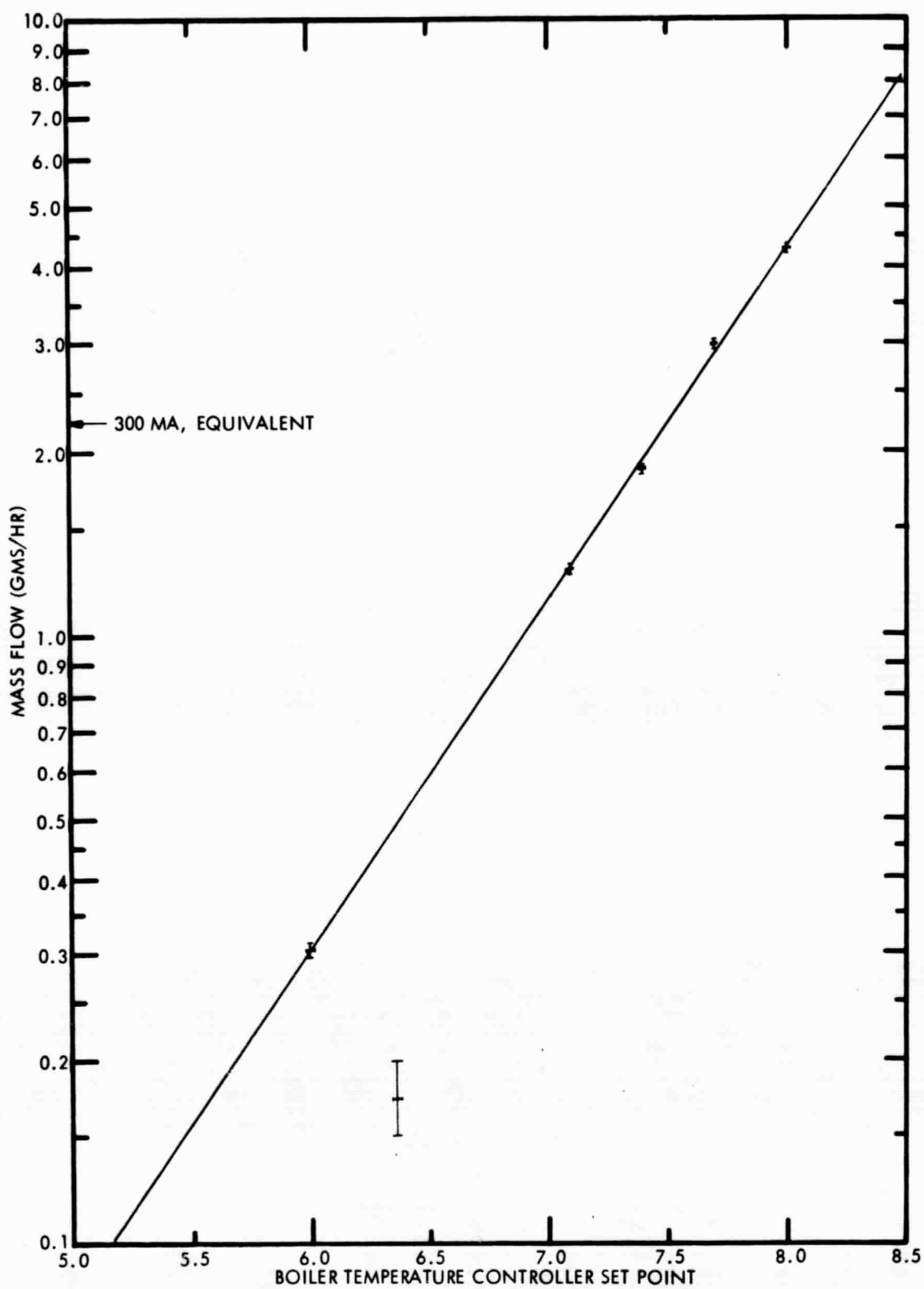


Figure 3. Mercury mass flow from engine boiler vs temperature controller set-point.

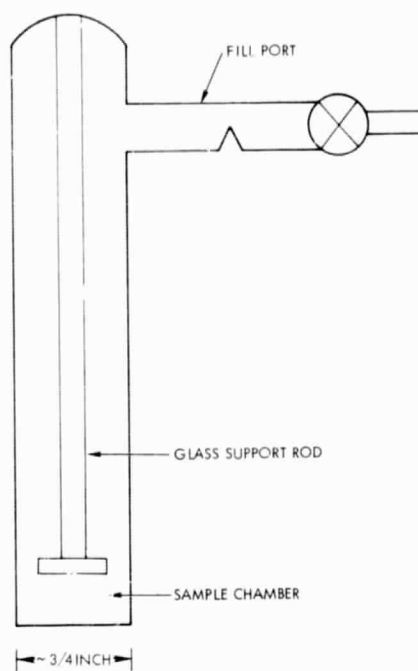


Figure 4a. Test vessel for metallurgical immersion tests.

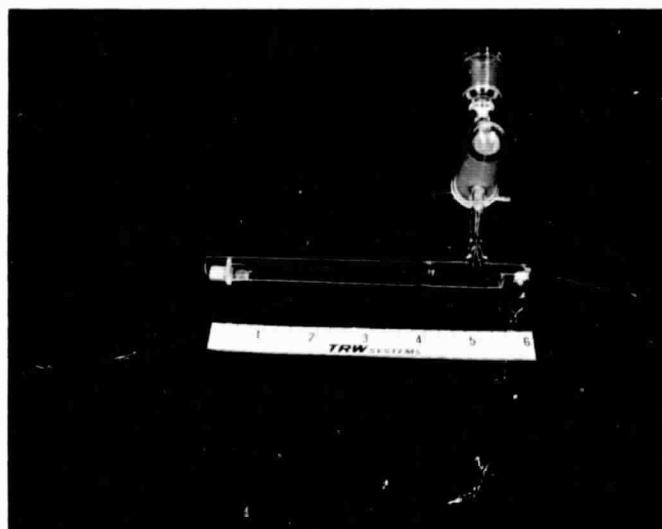


Figure 4b. Photograph of test vessel with solder sample loaded.

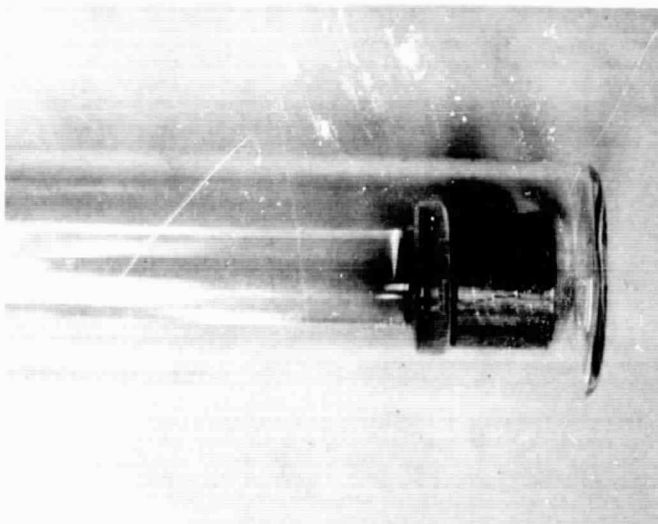


Figure 5a. Solder sample prior to addition of mercury.

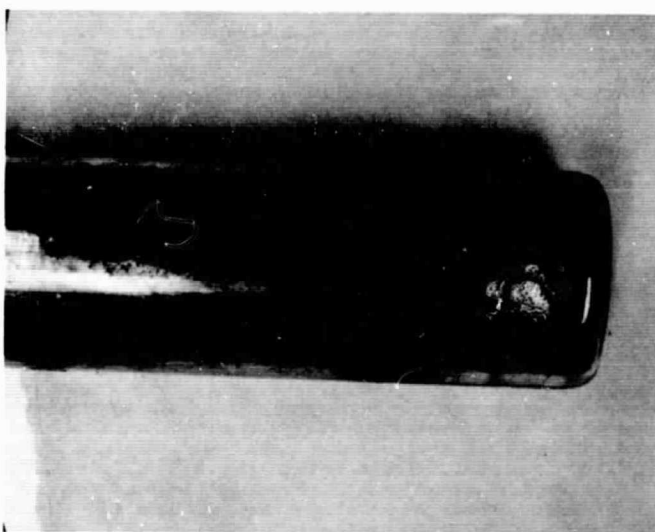


Figure 5b. Solder sample after one week exposure to mercury.

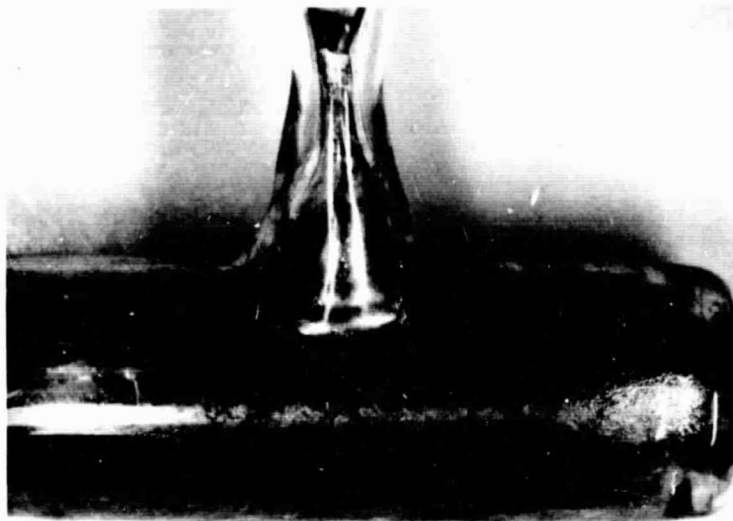


Figure 6. Photo of upper end of test vessel showing metallic deposit.

2. Future Work. During the forthcoming period, the mercury/silver and cesium/solder tests will be initiated. Mechanical and electrical tests for both materials in both propellants are being designed.

Information is needed from JPL to define the exact compositions of both the solder and of the silver so that these tests can be representative as possible of S/C materials of interest.

C. Thermophysics

1. Summary. This report covers the period from 10 February 1969 through 25 April 1969. During that period, sample materials were ordered and most of the samples were prepared, spectral distribution of the Christie solar simulator was measured under various conditions, a BASIC computer program was written for reducing the spectral data, one of the sample holder units was assembled and temporarily coupled to the controller and successfully

tested in vacuum with LN_2 surrounds, and the other four sample holder units were subsequently also assembled and mounted to essentially complete the five sample holder package. These tasks were performed on schedule but have required a somewhat higher level of effort in terms of man-hours than was originally expected. Only one potentially serious technical problem has emerged. The actual magnitude of that problem (spectral non-uniformity of the solar simulator beam) has not yet been fully assessed, but it appears that some fairly major changes in the Christie mounting structure may be required.

2. Sample Procurement and Preparation. The following table indicates the present status of the sample procurement program. It can be seen that sample procurement is essentially complete.

Table 1: Sample Procurement

Sample Material	Current Status
gold plating on 6061 T6 Alum.	30 Ready
polished 6061 T6 Alum.	30 Ready
Boeing Barrier anodized 6061 T6 Alum.	to be supplied by JPL
Corning 7940 quartz	30 discs received, Now applying VDA to all 30
Corning 0211 Microsheet	75 discs received, Now applying VDA to 30
PV 100 white paint on 6061 T6 Alum.	30 Ready
Z93 white paint on 6061 T6 Alum.	81 will be shipped 5/9/69 from IIT.
S13G white paint on 6061 T6 Alum.	81 will be shipped 5/9/69 from IIT.
Cat-a-lac black paint on 6061 T6 Alum.	30 Ready
3M 401-C10 black paint on 6061 T6 Alum.	30 Ready
RTV 566 on 6061 T6 Alum.	} Material not yet ordered
RTV 40 on 6061 T6 Alum.	

3. Christie Simulator Beam Measurements.

a. Beam Intensity Requirements. The method chosen to measure sample absorptance is to first elevate sample temperature above ambient with electrical power to the sample heater (which, in itself, permits calculation of emissivity) and then turn on the light beam and reduce the electrical power until the previous sample temperature is obtained. The reduction in electrical power is a measure of the light power absorbed by the sample. Obviously, the absorbed light power cannot be permitted to exceed the initial electrical power. If it did, the final sample temperature would exceed the initial sample temperature even with no electrical power input. On the other hand, the absorbed light power should be a significant fraction of the initial electrical power so that the change in electrical power is accurately measurable.

When these requirements are interpreted in terms of the wide range in α/ϵ among the various sample materials, the need for some control over light beam intensity is evident. Table 2 shows how the different types of sample materials can be grouped to achieve these conditions with three beam intensity levels.

It is presently planned that these beam intensity levels will be obtained by the following methods.

- (1) High Intensity. Preliminary radiometer measurements indicate that the Christie simulator when operating at the rated 65 amperes, will provide approximately the desired 151 mw/cm^2 if the beam is focussed down to cover a 10 to 11 inch diameter spot. This diameter will just cover the five samples and the reference radiometer.
- (2) Medium Intensity. The medium intensity beam will be obtained by introducing several layers of 60 mesh screen (woven from 7 mil brass wire) into the high intensity beam.
- (3) Low Intensity. The low intensity beam will be obtained by removing the lens system from the Christie and introducing a single layer of 60 mesh brass screen. Radiometer measurements indicate that this will result in an intensity of about 3 mw/cm^2 at the 4'8" test distance.

TABLE 2. ESTIMATED BEAM INTENSITY REQUIREMENTS

Sample Material	Anticipated (1) Properties			Anticipated Power (T=70 F, R=50Ω)			Anticipated Beam Intensity		Beam Heating Ratio
	α	ϵ	α/ϵ	P (mw)	E (Volts)	I (ma)	G (mw/cm ²)	G (Suns)	
Copper Tape	.47	.04	11.8	26.6	1.15	23.0	2.98	.0213	.815
Polished Aluminum	.35	.04	8.8	26.6	1.15	23.0	2.98	.0213	.638
Gold	.23	.02	11.5	13.3	0.82	16.3	2.98	.0213	.800
Anodized Aluminum	.89	.80	1.1	532.	5.16	103.	32.0	.228	.811
Cat-a-lac Black Paint	.95	.86	1.1	571.	5.34	107.	32.0	.228	.825
Z-93 White Paint	.15	.90	.17	597.	5.46	109.	151.	1.08	.588
S 13G White Paint	.20	.88	.23	584.	5.40	108.	151.	1.08	.600
0211 Microsh et	.14*	.80	.18	531.	5.14	103.	151.	1.08	.616
7940 Quart	.14*	.80	.09	531.	5.14	103.	151.	1.08	.616

* Back side vacuum aluminized

(1) Prior to degradation

b. Spectral Distribution Measurements. The spectral distribution of a Christie UXL-1600 xenon lamp in a Model UF30K lamphouse has been measured under various conditions to evaluate:

- o Spectral change with time
- o Spectral effect of introducing wire screen
- o Spectral effect of removing the lens system
- o Spectral effect of changes in electrical current
- o Spectral non-uniformity across the beam diameter
- o Spectral effect of changes in divergence angle

All measurements were made on the Beckman DK-2A Spectrophotometer using an NBS standard quartz iodide lamp (No. QM141) as a reference lamp. The spectral data was reduced and normalized on Tymshare software using a BASIC computer program which is described in a later section. The most interesting of the normalized spectral distribution and integral curves are plotted in Figures 7 to 12.

Results from the first series of tests (runs 1-5) were reported in the March progress report. They indicated that the spectral distribution changes rapidly during the first few hours of lamp life, but is essentially stable after 20-30 hours of operation. The main change during this "breakin" period was a reduction in the UV output, (apparently due to lamp envelope transmission degradation).

The second series of tests, (runs 6 and 7), was made in order to determine whether or not a wire mesh screen could be used to attenuate beam intensity as will be required in order to test samples of differing α/ϵ ratios at essentially constant temperature. Runs 6 and 7 were therefore made under almost identical conditions except that a single layer of 60 mesh screen woven from approximately 7 mil diameter brass wire was placed just ahead of the Christie housing during run 7. The results of this test and several auxiliary spectral transmission tests (made using the internal Beckman light sources rather than the Christie) indicate that the brass screen as used here has essentially flat spectral transmission. The slight effect that

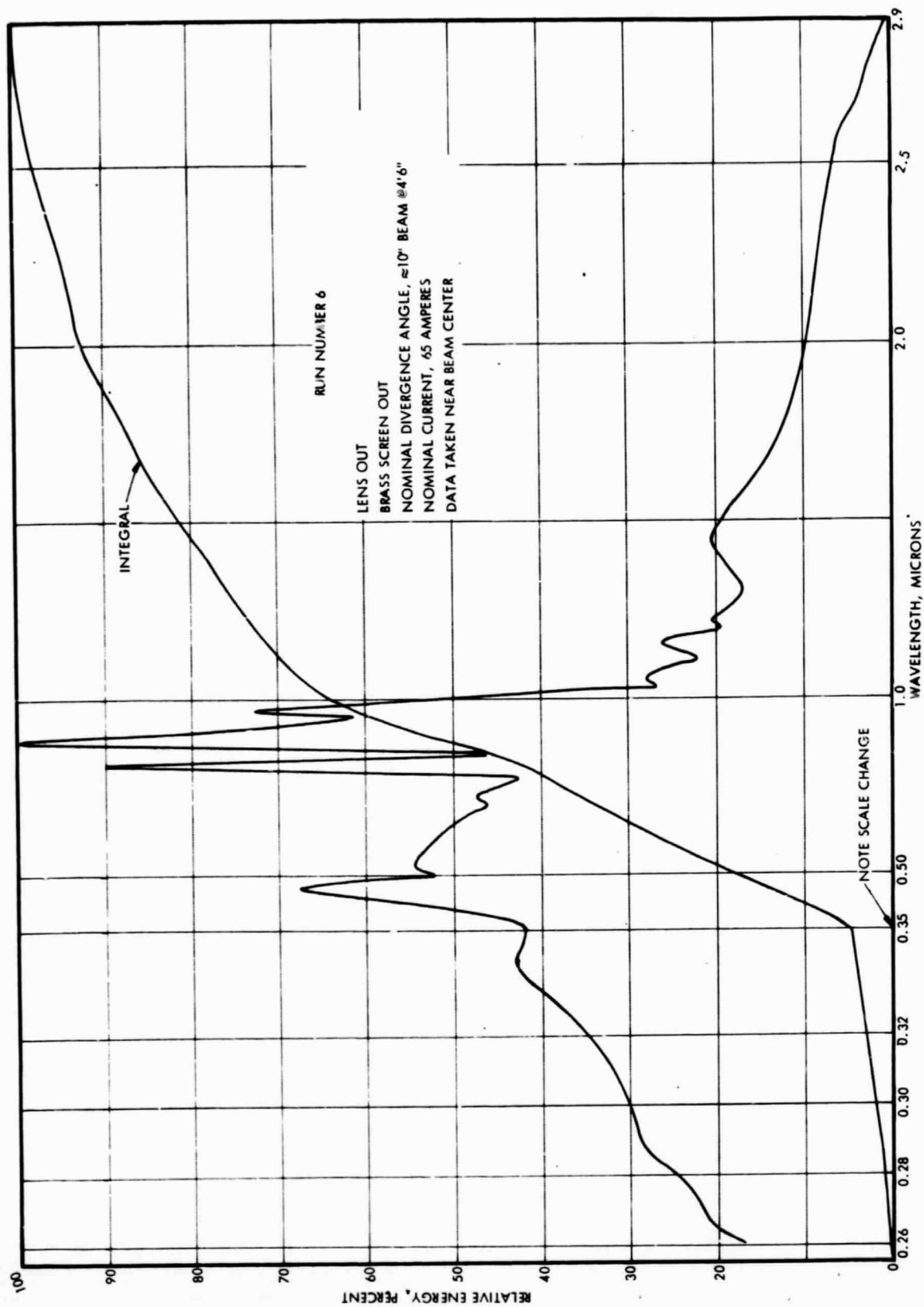


Figure 7. Normalized spectral distribution (and its integral) of solar simulator system.

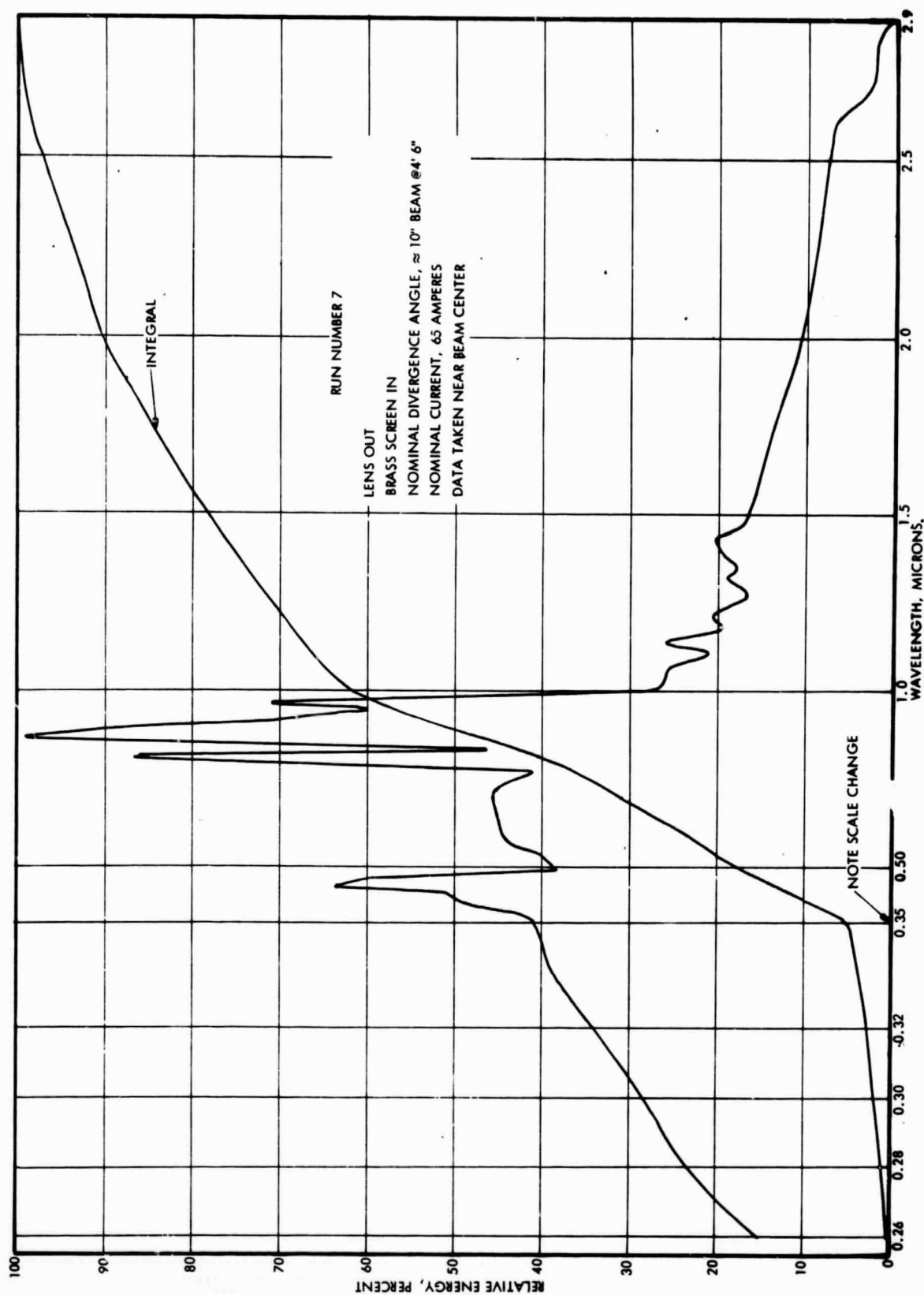


Figure 8. Normalized spectral distribution (and its integral) of solar simulator system.

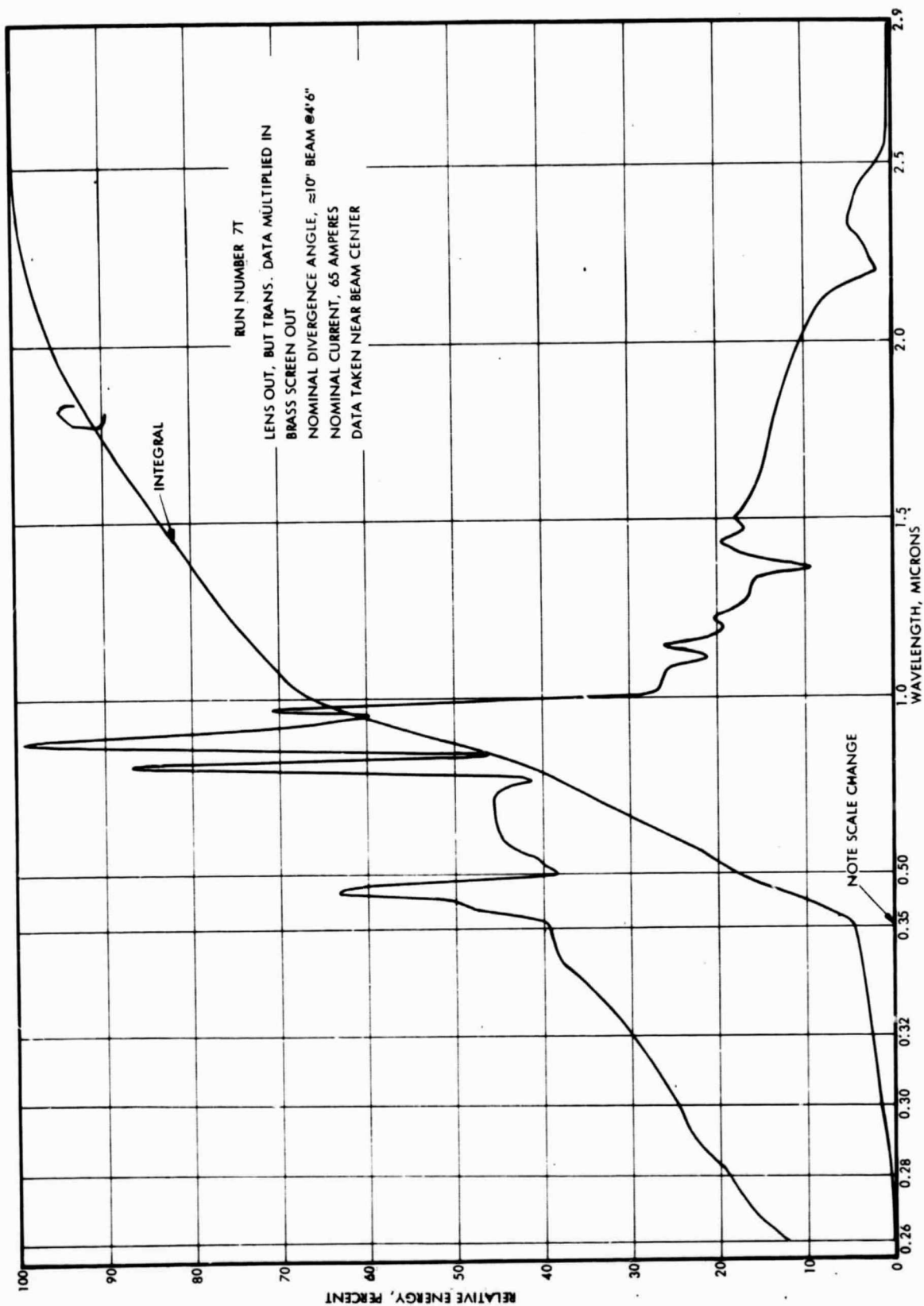


Figure 9. Normalized spectral distribution (and its integral) of solar simulator system.

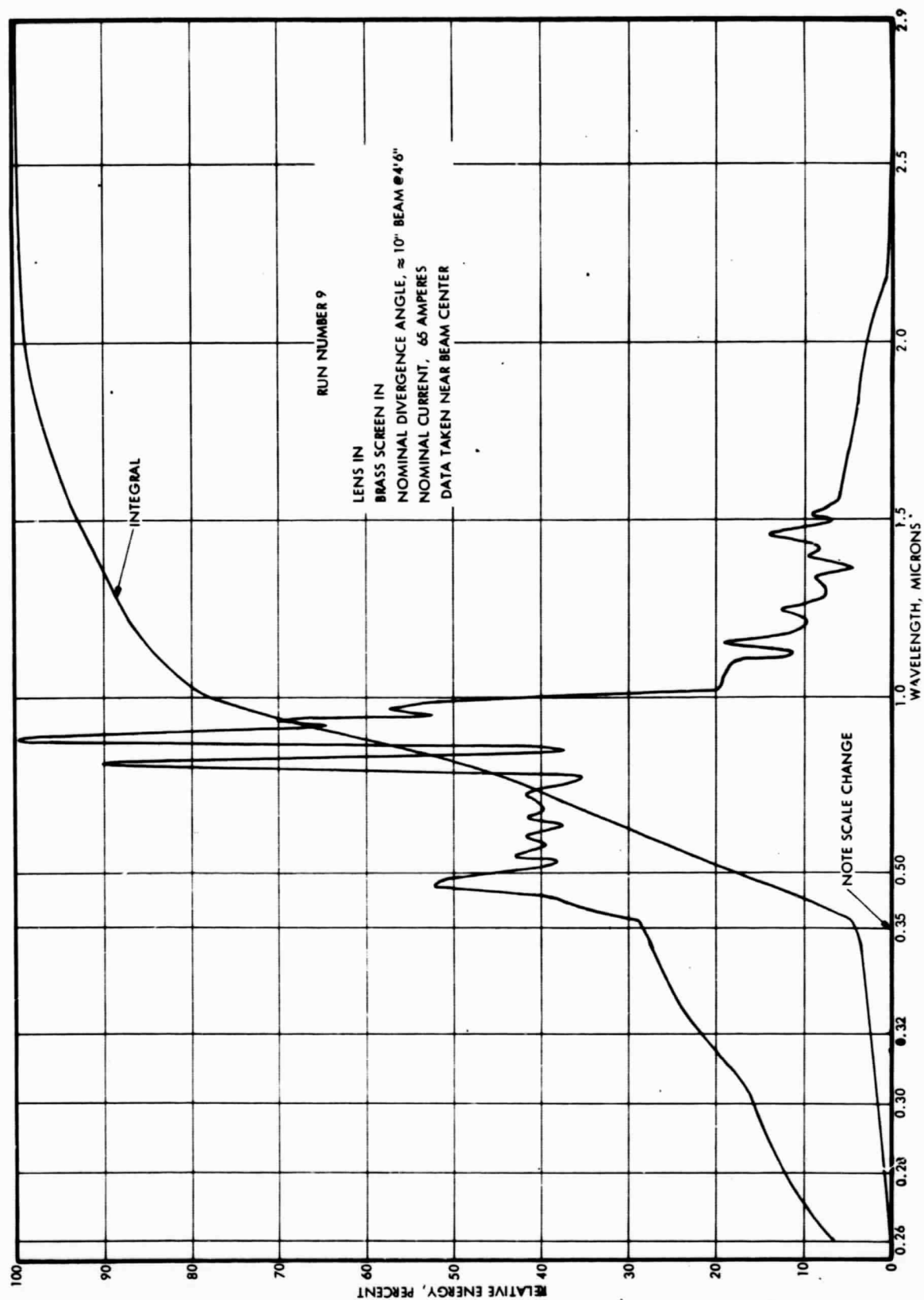


Figure 10. Normalized spectral distribution (and its integral) of solar simulator system.

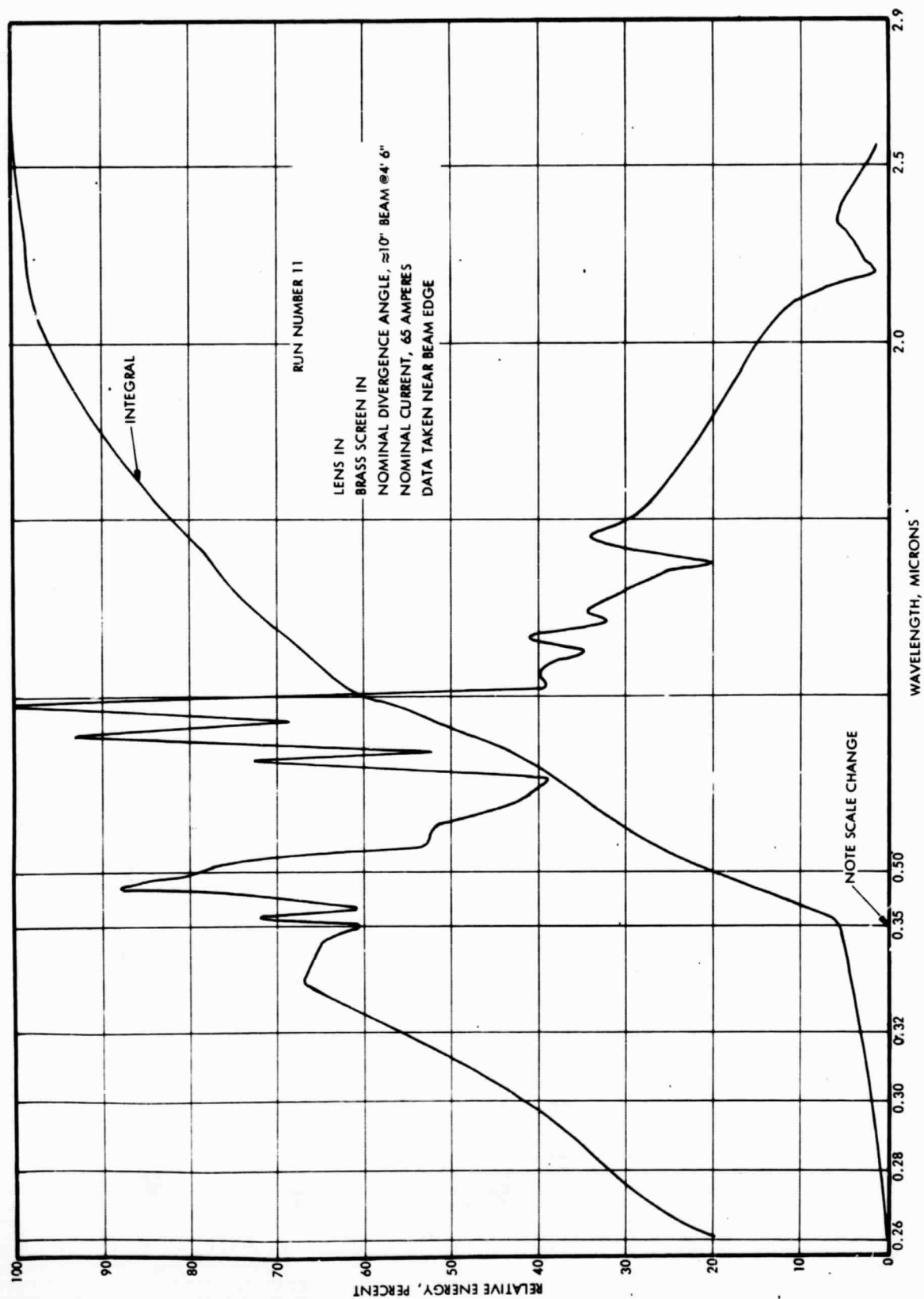


Figure 11. Normalized spectral distribution (and its integral) of solar simulator system.

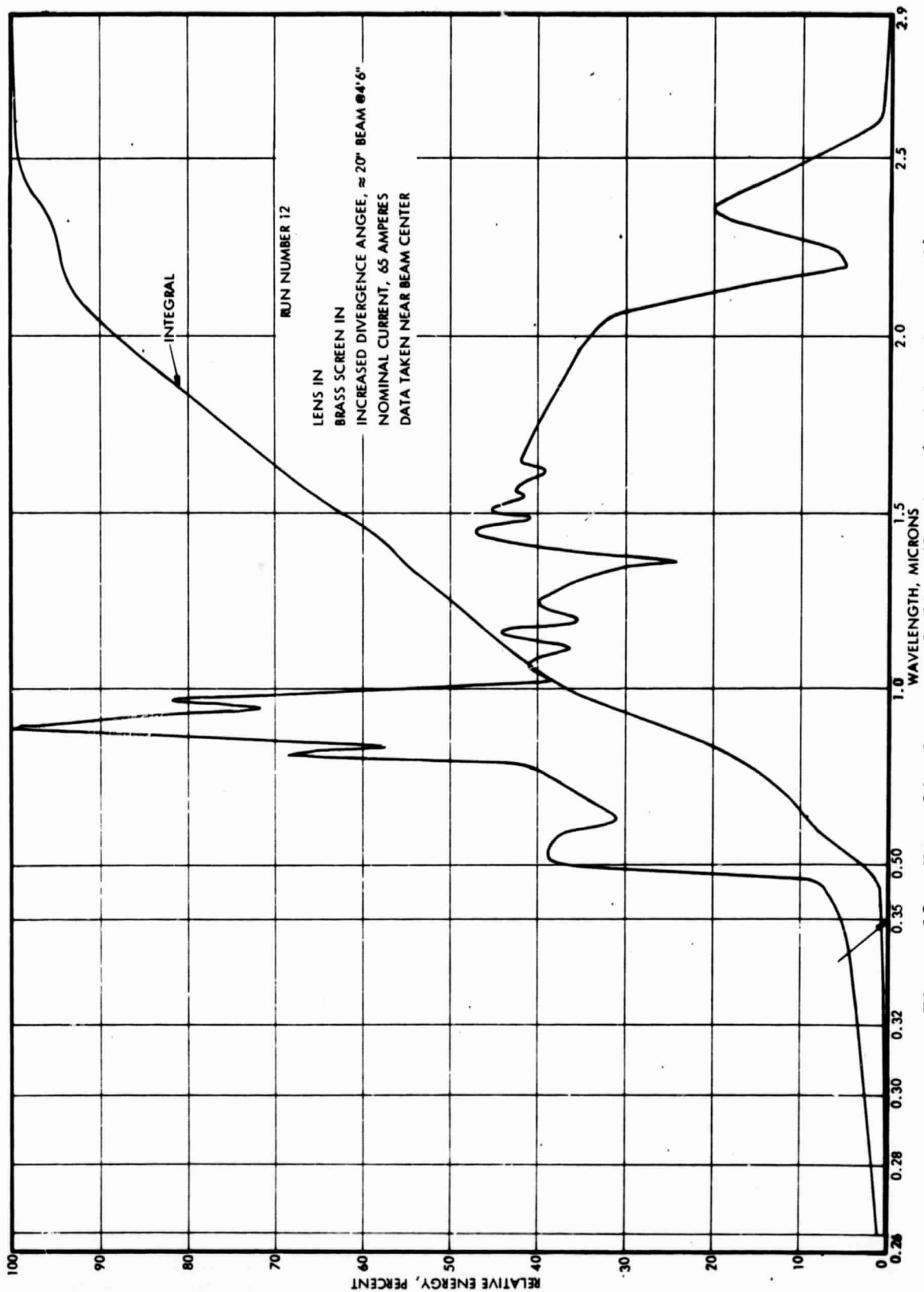


Figure 12. Normalized spectral distribution (and its integral) of solar simulator system.

it does impose can, if necessary, be accounted for when comparisons are to be made between in situ total data and ex situ spectral data. Comparisons between before-exposure and after-exposure in situ measurements will not be affected by the slight screen perturbation because both measurements will be made under the same conditions, (screen in or screen out).

The third series of tests was made in order to evaluate shifts due to the presence or absence of the lens assembly. This is important because it is anticipated that the lens assembly will be removed when testing samples with a high α/ϵ ratio (metals) in order to obtain very low beam intensity. The spectral distribution of the beam is affected in at least three ways by the lens assembly. First, the quartz elements have a somewhat non-uniform spectral transmission. This effect could be reduced or practically eliminated by introducing an equivalent thickness of quartz whenever the lens is removed. The second effect occurs because the lens tends to image part of the electrodes as well as the arc into the beam. The third mechanism is chromatic aberration of the lens system. A comparison between runs 9 and 7 indicates the total spectral change imposed by the lens assembly. A comparison of run 9 with run 7T indicates the change that remains if the transmission component is removed. Run 7T was obtained by multiplying the spectral data of run 7 by the spectral transmission data of the lens assembly (as measured on the Beckman during an auxiliary test) and renormalizing. From these comparisons, it appears that replacing the lens assembly with an equivalent thickness of plain quartz during low intensity runs will provide a spectral distribution that is acceptably similar to that obtained for high intensity runs (lens in, nominal divergence). This is particularly true since it is unlikely that the α/ϵ ratio of any given sample will ever degrade to such an extent that the sample would have to be tested after exposure at a different intensity level than it was tested in before exposure.

While electric current change has tentatively been ruled out as a method of intensity control because of the limited range available with the present power supply, it is of interest to know how sensitive the spectral

distribution is to inadvertent fluctuations in the current. For that reason, run number 10 (not presented here) was performed under the same conditions as run number 9 (Figure 10) except that the electrical current was dropped from 65 to 55 amperes. The resulting spectral distribution was almost identical to that of run 9.

By far the most disturbing finding in all of the spectral measurements was that the spectral distribution is significantly non-uniform across the beam diameter, at least when the lens is in place. This fact can be seen by comparing the results from run 11 taken near the beam edge with those of run 9 taken near the beam center. Although additional data would be needed for a conclusive statement, it is easy to imagine that the spectral distribution changes rapidly with position at outer sample locations. If so, beam alignment becomes very critical not only within the vacuum chamber but also in regard to correlating sample holder positions with Beckman measurement positions. Consequently, this matter is under study and several solutions to this likely difficulty are being considered. The most favored solution at present is to mount a telescopic sighting device on the Christie which would allow one to aim a single specific spot in the beam onto each sample position (or the Beckman sphere port) one at a time. This approach of course requires some kind of X-Y translation motion or angular rotation motion with fine control.

A final spectral distribution test (run 12) was made to determine how sensitive the spectral distribution would be to inadvertent changes in the beam divergence angle. This angle is changed by sliding the lens assembly in or out relative to the arc lamp. A comparison of the results of run 12 with those of run 9 indicates that the spectral distribution, particularly in the IR region is greatly affected by beam divergence angle. It will therefore be necessary to make provisions for positive indexing of the lens assembly so that it will have the same divergence angle everytime it is reinstalled.

4. Computer Program. A BASIC computer program has been written for reducing the spectral lamp intensity data. This program performs linear interpolation between input coordinate points representing up to four different curves. Each curve may have up to 100 input points. The program determines the x-coordinate (wave-length) range covered by all of the input curves and divides this common range up into any desired number of increments (up to 500). It then performs the desired operation increment by increment.

In the present case, the desired operation is to multiply the three curves together. The first curve represents Beckman data which is the ratio of energy from the xenon lamp to energy from the known reference lamp. The second curve is the spectral distribution data for the reference lamp. The third curve is spectral transmission data for a filter (may be made unity).

After the point by point calculations have been completed, the program normalizes with respect to the peak value of the product curve and prints out relative intensity versus wavelength and the percent of total energy lying below each printed wavelength.

This same program (with a minor change) will be used later to reduce ex situ spectral absorptance data in order to obtain the total absorptance relative to our xenon lamp spectrum or relative to the solar spectrum.

5. Sample Heating Unit Fabrication. .

a. Guard Heater Omission Decision. A decision was made to omit the guard heaters from beneath the heat flux meters to minimize the thermal resistance between the sample and the sink. The original reasons for using the guard heaters were:

- (1) To isolate the sample from sink temperature fluctuations.
- (2) To allow nulling of the heat meter without disturbing the main heater power and thus the power measurements.
- (3) To allow a certain amount of choice in the sample temperature during measurements without varying sink temperature. This would

permit constant light intensity, yet provide the flexibility to test varying α/ϵ samples on the same run. Thus a high α/ϵ sample could be operated at a higher temperature so that its emitted flux would exceed its absorbed flux, (a necessary condition), even for fairly high beam intensity required for low α/ϵ samples.

In regard to Item 1 above, the tap water temperature in building 01 was measured over a period of nearly a week. Variations were found to be $\pm 1^\circ\text{C}$ (1.8°F) but the rates of change were in general quite low so that during any given single measurement period sink temperature drift is expected to be far less than the accuracy of the measurement.

Concern over Item 2 was greatly reduced by preliminary tests with the automatic controller and an old sample heating unit operating in air. These tests indicated that the controller was stable and did not hunt or oscillate. The new heat flux meter units which have approximately the same sensitivity as the old ones are about 1/4 as thick as the old ones. Response time should therefore be faster and the closed-loop control will be even tighter than before. (The verification of these predictions are described in Section c below.) This improvement has been made possible by the acquisition of a new coil winding machine which allows finer wire to be handled and spaced approximately 4 times closer than before. More turns mean more output for a given area and thickness.

Moreover, the heat flux meters would be calibrated by testing with a black sample of known emittance. If controller stability did turn out to be a problem for low emittance samples, the electrical power could be turned off or held constant. The non-nulled heat flux meter would then be read and the heat flux could be computed from the calibration factor.

The present guard heaters have an estimated maximum power capability of about 30 watts each. In order to implement Item 3, this 30 watts must be capable of raising the temperature of a high α/ϵ sample several hundred degrees F. This is true because of the large difference in equilibrium

temperature between the various samples. For example, at 1.0 sun, gold ($\alpha/\epsilon \approx 11.8$) has an equilibrium temperature of about 860°F while Z93 white paint ($\alpha/\epsilon \approx .17$) has an equilibrium temperature of about 0°F. A thermal resistance of at least 300°F/30 watts or 10°F/watt should therefore be placed between the guard windings and the sink if a guard heater is used.

This resistance would cause an undesirable temperature rise during exposure to the ion engine exhaust. The heat flux density due to impingement of the ion engine exhaust may be as high as 1 watt/cm². Such a flux density would impose 15.5 watts on each sample package which would result in 155°F temperature rise through the required thermal resistor.

This rise plus the rise through the guard heater itself and its interface, plus the inescapable rise through the heat meter, main heater, and associated interface layers, would cause the sample temperature during exposure to be as much as 200°F above the sink temperature. Thus, unless the sink temperature were made variable over a wide range, the sample temperature would be a strong function of ion arrival rate and/or velocity. These are parameters which we want to vary independently of sample temperature. For this and other less important reasons, the guard heaters were omitted. All samples will therefore be exposed and tested at essentially sink temperature. This temperature could be varied by circulating tap water, or water from an ice bath, or water from a boiling bath. Sample temperatures can be varied a limited amount during exposure by applying power to the main heater. The necessary condition that emitted heat flux must equal or exceed absorbed flux will be met by varying the incident beam flux density.

b. Final Sample Holder Design. The 1-3/4 diameter sample holder design now consists of an 11-mil heat meter, a 5-mil copper foil, a 17-mil heater, and a 10-mil beryllium copper facesheet all bonded together in that order with RTV 165. The heat meter side of five such packages are bonded to a 1/8-inch thick water-cooled copper plate. The total package thickness from the mounting surface on the heavy copper plate to the far side of the beryllium copper facesheet is approximately .062 to .068 inch.

The purpose of the 5-mil copper foil that has been added between the heat meter and the heater is to prevent a few heat meter junctions which might otherwise happen to fall close to heater wires from being overly influential.

A 1-mil chromel-alumel thermocouple is soldered to the back side of each beryllium copper facesheet. Lead wires from this thermocouple and from the heater and heat meter go straight back through small holes in the 1/8-inch thick copper sink plate to stand-off terminals on the back side. Thus, the annular phenolic terminal strips originally planned for the front side have been eliminated. This change was made in order to simplify construction and allow reduction in the size of the ion shield which will surround each sample holder package. The 38-gauge constantan heater leads running between each heater and the stand-off terminals (where the voltage is measured) were silver plated and twisted around a 30-gauge copper lead in order to reduce lead resistance to a negligible fraction of the heater resistance. The total heat leak due to thermal conduction along the lead wires is expected to be acceptably small, since there will never be more than 1 to 2°F temperature gradient along the leads during the measurement period.

c. Preliminary In Situ Test. The center sample holder unit was assembled and mounted to the sink plate for a preliminary test in vacuum before the other four units were assembled. This test was conducted so as to be sure that the new design with the 5-mil copper foil, thinner heat meters and no guard heaters would null satisfactorily and remain stable with the automatic controller driving the main heater.

A LN_2 cooled shroud within an approximately 19 inch diameter vacuum chamber provided the desired environment, and tap water was circulated through the mounting plate tube. A 1.75 inch diameter .016 inch thick aluminum disk coated with Cat-a-Lac black paint was bonded to the sample heater face with quick-cure RTV-11 to serve as a sample. The emissivity of the sample was measured on the QED (quick emittance device), prior to mounting and was found to be 0.89.

Unfortunately, the ion shields had not yet been machined at the time the test was run. Consequently, the sample and heater edges were exposed full view to the LN_2 surrounds. The resulting heat loss from the edge caused a slight discrepancy between the measured electrical power (0.581 watt) dissipated in the heater, and the emitted power (0.543 watt) calculated from the known emissivity and the measured sample temperature. The following two tables summarize the data obtained during the test.

TABLE 3. CONTROLLER TURNED ON

Heater face temperature	61.4°F
Mounting plate temperature	62.1°F
Heat meter output	null \pm 4 μV
Heater voltage	5.305 volts
Heater current	0.1095 amperes
Heater power (measured electrically)	0.581 watts
Emitted power (calculated for sample face)	0.542 watts

TABLE 4. CONTROLLER TURNED OFF

Heater face temperature	58.4°F
Mounting plate temperature	62.0°F
Heat meter output	2.1 mv
Emitted power (calculated for sample face)	0.532 watts

As indicated in Table 3, the controller maintained the heat meter within about \pm 4 μV of null. This is considered to be excellent control and stability. Table 4 indicates that 0.532 watts of heat flow, (neglecting edge loss), produced 2.1 mv of output on the heat meter. The apparent sensitivity of the heat meter is then approximately 3.95 mv/watt. From this fact, it would appear that the \pm 4 μV of heat meter imbalance in Table 3 represents about \pm 0.001 watt of heat flow through the meter. This is considered to be an acceptably low uncertainty.

Table 4 also shows that 0.532 watts of heat flow through the package produced a temperature difference of approximately 3.6°F between the mounting plate and the heater face. The apparent thermal resistance of the package, (not including the sample to heater interface resistance), is then approximately 6.77°F/watt. Thus even with the thinned down design, an incident heat load of 1 watt/cm² (as may occur during exposure to the ion engine) over a sample area of 15.5 cm² may produce sample temperatures as much as 105°F above the mounting plate temperature. This is no problem from a materials standpoint but, as pointed out earlier, may cause the sample temperature to be a function of ion arrival rate and/or velocity. If so, the choice is between accepting a variety of exposure temperatures as ion parameters are varied from run to run, or controlling sink plate temperature.

During the tests, it was found that the stabilizing process in going from steady state with the controller off to steady state with the controller on took only about five minutes. The 90% time constant calculates out to be about 100 seconds. It thus appears that with such fast response, there will be no need for the holding circuits which originally were to be manually adjusted to keep the four sample units not connected to the controller at an approximate null.

d. Fabrication Schedule. Fabrication work on the surface thermal sample holder package is essentially complete except for mounting the ion shields. The five heater-heat meter units have been assembled, mounted on the plate and wired with six-foot leads. These leads will be connected to the hermetic seal passthrough as soon as the passthrough is received. The shields have been machined but must be modified slightly and then custom fitted to each of the five sample units. There are also several details still to be completed such as soldering the cooling tube joints.

Work has also begun on construction of the switching and control console that will operate the sample heating units. This will consist of a rack mountable enclosure that will house the necessary switching circuits, the automatic controller (already built), and the Hewlett

Packard microvolt amplifier that drives the controller. All of this work is expected to be completed before June 1st.

6. Work Planned for Next Period. Tasks which are expected to be completed during the next reporting period are:

- (1) Fabrication details on the sample holder unit.
- (2) Fabrication of the control console and switching circuits.
- (3) More spectral distribution measurements will probably be made on the Christie simulator beam. The specific nature of these measurements depends on what course of action is decided upon concerning the spectral non-uniformity across the beam.
- (4) Relative intensity measurements will be made with a radiometer placed alternately at the five sample positions and then at the reference radiometer position within the chamber. These measurements also must wait until the decision mentioned in (4) is made.
- (5) Ex situ measurement of the samples.

D. Chemistry

1. Cesium Immersion Tests. Kapton film was chosen as the first material for chemical evaluation as Kapton is the major plastic construction material for the 30 watt/lb General Electric roll-up solar array concept.

2. Kapton, Initial Immersion Test. A one liter resin kettle was fitted with a lid sealed with Apiezon wax and connected to a vacuum system consisting of a roughing pump, and LN_2 cooled trap. The system was evacuated to 25 μ and the kettle was heated to approximately 100°C and held overnight to insure drying of the glass.

The following morning the resin kettle, still evacuated, was transferred to a dry box, along with the Kapton film and cesium to be used in the experiment. The entrance chamber of the dry box was evacuated to $\sim 1 \mu$, and held there for one hour and then back filled with high purity argon.

The kettle was opened to the argon atmosphere and the sample was placed inside of it, followed by enough cesium to immerse the film completely. The kettle was taken out of the dry box, evacuated to $25\ \mu$, and stored at room temperature for 24 hours. At the end of this time, the kettle was replaced in the dry box and the sample was withdrawn and quenched with methanol.

During the withdrawal of the film, it tore into several fragments, and after quenching it was noted that the tear strength was almost nil.

It was thought possible that the Kapton film may not be entirely water free using the above experimental method and thus the film decomposition may have been due to the reaction of cesium hydroxide with Kapton rather than cesium metal. An improved apparatus was designed which allows exposure of very dry materials to distilled cesium metal at the temperature of choice.

3. Improved Apparatus. The improved apparatus was designed (Figure 13) and assembled. It allows anhydrous and oxygen free exposure of samples to distilled cesium.

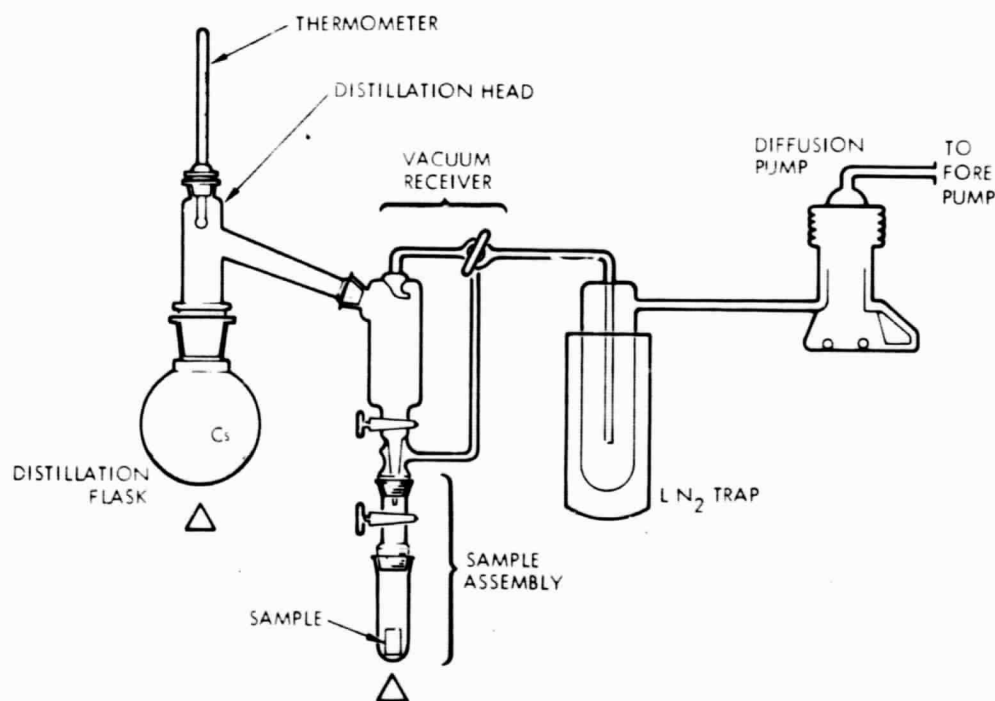


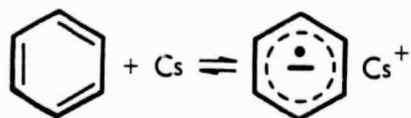
Figure 13. Cesium distilling apparatus

Operation.

- (1) Apparatus is placed in under a vacuum of 25 microns.
- (2) Sample is dried by heating to 70°C for 2 hours.
- (3) Cesium is distilled (240-250°C) onto sample (at temperature of choice), covering sample.
- (4) Sample assembly is removed, still under vacuum, and transferred to a glove box where it is stored for duration of exposure.
- (5) Sample is removed from assembly in glove box and immediately immersed in quench solution.

4. Kapton, Immersion Test. The improved apparatus and procedure described above was utilized to expose well dried Kapton film to distilled cesium. The film was exposed to cesium at room temperature for a period of forth-eight hours. The film rapidly turned to a dark purple color where exposed to cesium, but after removal of the film from the cesium environment and quenching (destruction of cesium) the tensile strength of the film had not changed (25,000); in addition, chemical analysis of the quench solution by thin layer chromatography showed that no organic portion of the Kapton film had been chemically reacted. The formation of the purple color, however, is highly significant.

Aromatic organic compounds (those containing phenyl or fused phenyl rings) form one electron oxidation reduction salts with strong alkali metal reducing agents such as sodium, potassium and lithium as shown in the figure for cesium:



These salts are highly colored due to low energy electronic transitions which become possible by virtue of the one electron oxidation reduction reaction. The salts are semiconductors, whereas the original polymeric

structure may have been an excellent insulator. Resistivities of the order of 10^1 to 10^{13} ohm·cm are common for these complexes in the dark or feeble light and many of them exhibit photoconductivity, where the resistivity may be lowered by an additional order of magnitude on exposure to visible light. Thus, it is contended that while the Kapton film is not chemically degraded, the one electron oxidation reduction salt is formed and it can be expected that the dark and light conductivity of the film will be increased by several orders of magnitude. This type of behavior, previously uninvestigated in the case of cesium, can be expected to be a factor in the case of any organic spacecraft material which contains aromatic nuclei (e.g. Epon 934, GT100, the RTV's, Cat-A-Lac Black, PV100 etc.). This is in addition to any two electron chemical reactions which may take place according to the individual structure of organic material. One measure of the extent to which the equilibrium shown above has taken place, is the number of free electron spins measureable per gram of material on exposure to cesium. In order to get a feel for this equilibrium, an attempt will be made to obtain an electron spin paramagnetic resonance spectrum on a Kapton-cesium mixture.

In order to evaluate the worst case effect of cesium on the Kapton film, a sample will be exposed at 50 to 60°C for a period of 48 hours.

5. Evaluation of General Electric array polymeric materials with regard to use in cesium and mercury ions and neutrals environment. A list of eight polymeric materials was evaluated on the basis of structure reactivity relationships with regard to use in cesium and mercury neutral and ion environments. The spacecraft materials are: Epon 934, Kapton-H film, Delrin, Sylgard-182, RTV-560, SMRD 745, Epiall 1914 and GT-100. Phone calls directly to a number of potential suppliers of each of the materials were made in order to identify, (1) the manufacturer, (2) the approximate structure of the polymeric material, and (3) in order to obtain samples where available. It was determined that SMRD 745 (G.E.) and Epon 934 (Shell) were epoxy polymers, Epiall 1914 (Allied) is an epoxy novolac-amine cured molding compound, Delrin (Dupont) is a polyacetal, GT-100 (Schjeldahl) is a polyester and Sylgard 182 (Dow Corning) is a polydimethylsiloxane with vinyl groups cured

with platinum and silane materials. The RTV and Kapton film have previously identified. The projected chemical effects of cesium neutrals on the polymeric materials are shown in Table 5.

III. CONCLUSIONS

The program is progressing satisfactorily through the initial fabrication and experimental phases in each of the four work unit areas.

An unexpected difficulty has been encountered in implementing the experimental design for in situ measurement of α and ϵ . Spectrographs of the xenon lamp output show important variation in spectral distribution with transverse position within the beam. Several possible solutions to this problem are under study.

Immersion of Kapton in liquid cesium has raised questions regarding their compatibility. If the Kapton is completely dry, a purple, one electron oxidation reduction, semiconductive, photoconductive salt layer is formed. In addition to this reaction, if residual water is present in the Kapton, as might be the case for several hours following array unrolling, liquid cesium seriously reduces Kapton's tensile strength. These are not desirable properties for solar cell substrates.

Immersion of soft solder in liquid mercury results in visible attack of its surface.

Further work is planned in each of the above mentioned areas.

IV. RECOMMENDATIONS

None

V. NEW TECHNOLOGY

None

TABLE 5. CHEMICAL EFFECTS OF CESIUM, CESIUM IONS, MERCURY, AND MERCURY IONS ON SPECIFIED SPACECRAFT MATERIALS

SPACECRAFT MATERIAL	CHEMICAL STRUCTURE	CESIUM	CESIUM ION	MERCURY	MERCURY ION
Kapton H-film	polyimide	extensive oxidation-reduction salt formation			
Epon 934	aromatic epoxy	oxidation-reduction salt formation	"	"	"
Delrin	polyacetal	very minor degradation	"	no reaction	"
Sylgard 182	polydimethylsiloxane with cured vinyl side groups	"	"	"	"
RTV-560	polymethylphenylsiloxane	oxidation-reduction salt formation	"	weak oxidation-reduction salt formation	"
SMRD 745	aromatic epoxy	"	"	"	"
EPIALL 1914	epoxy novolac	possible severe degradation	"	"	"
GT 100	polyester	oxidation-reduction salt formation	"	"	"

VI. REFERENCES

1. First Quarterly Letter, #08965-6004-R000, Contract NAS7-575
2. Second Quarterly Letter, #08965-6007-R000, Contract NAS7-575
3. Third Quarterly Letter, #08965-6010-R000, Contract NAS7-575
4. Final Report NAS7-575, Now in review.
5. AIAA Preprint 69-271